ACS APPLIED MATERIALS & INTERFACES

Research Article

www.acsami.org

Fluorographene with High Fluorine/Carbon Ratio: A Nanofiller for Preparing Low-κ Polyimide Hybrid Films

Xu Wang, Yunyang Dai, Weimiao Wang, Mengmeng Ren, Baoyin Li, Cong Fan, and Xiangyang Liu*

State Key Laboratory of Polymer Materials Engineering, College of Polymer Science and Engineering, Sichuan University, Chengdu, Sichuan 610065, China

Supporting Information

ABSTRACT: Sufficient amounts of fluorographene sheets with different sheet-size and fluorine/carbon ratio were synthesized for preparing of fluorographene/polyimide hybrids in order to explore the effect of fluorographene on the dielectric properties of hybrid materials. It is found that the fluorine/carbon ratio, width of band gap, and sheet-size of fluorographene play the important roles in determining the final dielectric properties of hybrids. The fluorographene with high fluorine/carbon ratio (F/C $\approx$ 1) presents broaden band gap, enhanced hydrophobicity, good dispersity and thermal stability, etc. Even at a very low filling, only 1 wt %, its polyimide hybrids exhibited drastically reduced dielectric constants as low as 2.1 without sacrificing thermal stability, improved mechanical properties obviously and decreased water absorption by about 120% to 1.0 wt %. This provides a novel route for improving the dielectric properties of materials and a new thought to carry out the application of fluorographene as an advanced material.

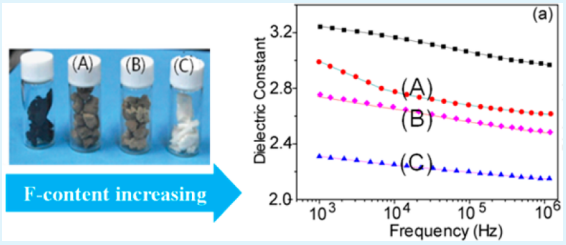

KEYWORDS: *fluorographene, semiconductor, dielectric constant, polyimide, hybrid, water absorption*

1. INTRODUCTION

The controlling of dielectric properties has attracted ever-increasing attention for preparing new type advanced materials with wide range of applications in electronic and electrical industry.[1−5] Thereinto, low dielectric materials have been one central interest because their utilization in integrated circuits can lower line-to-line noise in interconnects and alleviate power dissipation issues by reducing the capacitance between the interconnection conductor lines.[4,5] Polyimides have been widely used for dielectric applications, but their dielectric constant (κ, $3 < \kappa < 4$) and water absorption (~2 to 4%) are still not low enough as an alternative to traditional insulators such as silicon dioxide for future devices.[6−8] Initially, the introduction of controlled porosity in polyimides was envisioned as a promising method for developing low-κ materials in view of the low dielectric constant of air.[9−12] However, the mechanical strength of the resulting nanoporous film is weak and the Young's modulus is only in the range 0.4−0.6 GPa.[12] To keep the excellent mechanical properties, there are main two routes for decreasing their dielectric constant. One is the synthesis of fluorinated polyimide. The electronic polarization is always lowered with fluorine substitution because of the smaller electronic polarizability of the C−F bond relative to C−H, which can reduce the dielectric constant. However, most reported examples of fluorinated polyimide are in the range of dielectric constant between 2.6 and 3.0 and need complicated synthesis processes. For another route, some porous nanoparticles with stiff structure, such as porous polyhedral oligomericsilsesquioxane (POSS), silica nanotubes, and polyoxometalates have been introduced.[12−17] The addition of inorganic components results in loose stacking of the macromolecules surrounding solid particles, increasing of the free volume and decreasing of the dielectric constant of materials.[18−20] Nevertheless, the route always needs a large filling (about >10%) and increases the water absorption, which seriously affects the performance of hybrid polyimide films, including electrical properties and environmental adaptability. Thus, it is still an urgent issue to create the new routes for the preparing of excellent polyimide materials with low dielectric constant and low water absorption simultaneously.

Fluorographene, as one of the two-dimensional derivatives of graphene, is in the spotlight.[21−25] Due to inheriting the structural features of graphene and carbon material fluorides, fluorographene presents a series of novel interfacial and physicochemical properties, which brings a wide prospect in different fields for applications.[26−29] Several groups and ours have confirmed that the high fluorine/carbon (F/C) ratio equipped the fluorographene sheets with broaden band gap, enhanced hydrophobicity, and thermal stability.[21−23,30] Thus, it is expected that these characteristics carry amazing influence in the dielectric performances of the fluorographene composites such as dielectric constant, water absorption, and so on. However, the insufficient preparation methods of fluorographene with high F/C ratio have been hindering its development as the advanced materials, especially as the nanofiller for preparing of composites. Fortunately, our recent work first

Received: July 1, 2014
Accepted: September 1, 2014
Published: September 4, 2014

   dx.doi.org/10.1021/am5042516 | ACS Appl. Mater. Interfaces 2014, 6, 16182−16188

reported the synthesis of the fluorographene sheets with high F/C ratio (F/C = 1.02) and few layers (mainly in the 1- to 5-layer range) in large scale by direct fluorinating of graphene oxide.[30] Here, we synthesized sufficient amounts of fluorographene sheets with different fluorine content, size, and layer number by modifying the fluorination method and prepared the corresponding fluorographene/polyimide hybrid in order to find the effect of fluorographene sheets on the dielectric properties of hybrid material.

2. EXPERIMENTAL SECTION

2.1. Preparation of Spongy Graphene (SG). Graphene oxide (GO) was prepared by the modification of Hummers's method from flake graphite (average particle diameter of 4 μm, 99.95% purity, Qingdao Tianhe Graphite Co. Ltd., Qingdao, China).[31,32]

A 2 wt % GO suspension in water was prepared. The aqueous solution of GO was loaded into square aluminum molds. The specimens were then plunged into liquid nitrogen, then dried in a freeze drier for 2 days. Finally, the samples were further dried at 80 °C for 2 h. The spongy graphene oxide (SGO) was prepared.[31,32]

Spongy GO (100 mg) was placed in a Petri dish set in a vacuum desiccator, where a piece of filter paper saturated with the chemical reducing agent hydrazine (80 wt % water solution, 5 mL) was placed in the desiccator for the reduction. The reducing reaction time is 72 h, and this sample was called spongy graphene (SG).[33]

2.2. Direct Heating-Fluorination of SG. The fluorination was carried out in closed stainless steel (SUS316) chamber (10 L) equipped with vacuum line. SG (100 mg) was put in the chamber. After exchanging nitrogen three times, we removed residual oxygen and moisture in the chamber. F_2/N_2 mixed gas (50 KPa) was introduced in to the chamber at room temperature (RT). Fluorination proceeded with the temperature increasing from RT to a certain temperature (room temperature, 180, 200, and 210 °C) at rate of 4 °C/min, and steady at this temperature for 180 min. The fluorination temperature was adjusted to obtain products with different degree of fluorination. The corresponding product was denoted as FSG-1, FSG-2, and FSG-3 for 180, 200, and 210 °C, respectively. Residual F_2 and byproducts in the chamber were removed at once by vacuum and absorbed by alkali aqueous solution. Then, fluorinated samples were taken out and preserved in dry atmosphere.

2.3. Preparation of Polyimide Hybrids with GF. The obtained 10 mg FSG was ultrasonic dispersed in 2 mL NMP under 300 W for 90 min, getting stable GF dispersion, which was added into 10 g prepared 10% solid content poly(amic acid)s solution of 3,3′,4,4′-biphenyl tetracarboxylicdiandhydride/4,4′-diamino diphenyl ether-system (BPDA/ODA). The mixture was stirred at room temperature for 2 h. Then, the solution was cast on a glass substrate and thermally processed (80 °C for 2 h; 140 °C for 1 h; 220 °C for 1 h; and 300 °C for 1 h). The hybrid films of fluorographene/polyimide with thickness in the range 18−22 μm were prepared for studying of dielectric, mechanical, and thermal properties. The content of fluorographene samples in the hybrids is 1.0 wt %.

2.4. Characterization. The surface chemical composition of fluorinated and nonfluorinated samples was examined by XPS with monochromatized Al Kα rays (1486.6 eV) under the circumstance of 12 kV × 15 mA, Kratos, Inc., at RT and at 2 × 10^{-7} Pa. Binding energies were referenced to the hydrocarbon peak at 284.8 eV. The takeoff angle was 20° with sampling depths of approximately 6−10 nm. AFM was carried out with a NanoScopeMultiMole & Explore from Vecco Instruments, using tapping mode. Scanning electron microscopy (SEM) and EDX was performed with FEI InspectF (FEIcompany, U.S.A.). The contact angle of water was tested using drop sharp analysis with 100 Krüss autovisual contact angle test equipment. Thermogravimetric analysis (TGA) was performed on Netzsch 209 TG instruments. Dynamic mechanical analysis (DMA) was performed on a TA Instruments DMA Q800under N_2 atmosphere, scanning from room temperature to 420 °C at a heating rate of 10 °C/min, the load frequency applied was 1 Hz. The dielectric constants measurements were conducted at room temperature, frequency range 1000 Hz to 1.2 × 10^6 Hz, and relative humidity 50%, using a broadband dielectric spectrometer Agilent 4294A. Optical pictures of neat polyimide films and hybrids containing FSG-3 under the transmissive mode were obtained by a Leica DMIP polarizing light microscopy with a Canon Power Shot 550 digital camera.

3. RESULTS AND DISCUSSION

3.1. Chemical Structure and Properties of Fluorographene. Fluorographene was synthesized from spongy graphene (SG) by direct fluorination with using fluorine gas as fluridizer, and the F/C ratio of fluorographene was adjusted by changing the fluorinating temperature. After fluorination, the alveolate structure is retained (Figure 1). Here, three kinds of

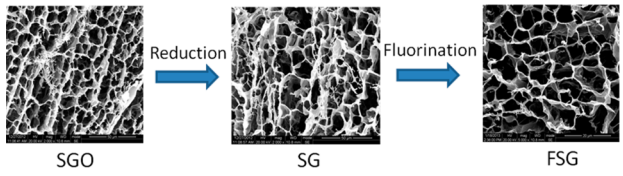

Figure 1. SEM pictures of SGO, SG, and FSG. After reduction and fluorination, the samples still retained the alveolate macropore.

fluorographene, FSG-1, FSG-2, and FSG-3, and the pristine SG are shown in Figure 2a. The color of samples changes gradually from black to gray to white with increasing of fluorination temperature.

The XPS data in Table 1 show that the value of F/C ratio of FSG-1, FSG-2, and FSG-3 respectively is 0.60, 0.78, and 1.00, increasing with fluorination temperature. Corresponding C 1s peaks of XPS spectra were also investigated in Figure 3. The C 1s curve fit spectrum of fluorinated samples exhibits three components corresponding to fluorine related groups, peak 4 at about 289 eV, peak 5 at about 291 eV, and peak 6 at 293 eV, which are assigned to CF_1, CF_2, and CF_3, respectively. The CF_2 and CF_3 groups are formed at the edge or the new defects of fluorographene sheet. The attack of fluorine inevitably brings defects into the graphene sheets during flluorination.

In the FTIR spectrum of SG (Figure 4), the absorption of the oxygen related groups disappeared after reduction of graphene oxide. In the process of fluorination, fluorine atom is covalently bonded to carbon atom of graphene. The absorption band at around 1220 cm^{-1} is assigned to the stretching vibration of covalent C−F bonds. With the increased value of F/C ratio, intensity of the band at 1220 cm^{-1} increases while that of the stretching vibration absorption of —C═C— and benzene ring respectively at around 1510 and 1610 cm^{-1} decreases obviously and even disappears in the spectrum of FSG-3. This is confirmed by the XPS data, and the —C═C— content (peak 1 in Figure 3, at about 284.5 eV) has decreased with rising of fluorination level. The conjugated groups are gradually fluorinated, resulting in the changing of color from black to white.

The introduction of oxygen is due to the residual of oxygen gas in the mixture of F_2/N_2 and replacement of F in C−F bonding by H_2O in the external environment, and a new oxygen related group is observed in the fluorographene, as the FTIR spectra of fluorinated sample all have the absorption peak at around 1840 cm^{-1}, which is attributed to the −C(O)F group. The XPS and FTIR results show that the composition of FSG-3 with the highest F/C ratio in this study is close but not stoichiometric, even though the value of F/C ratio is about 1.

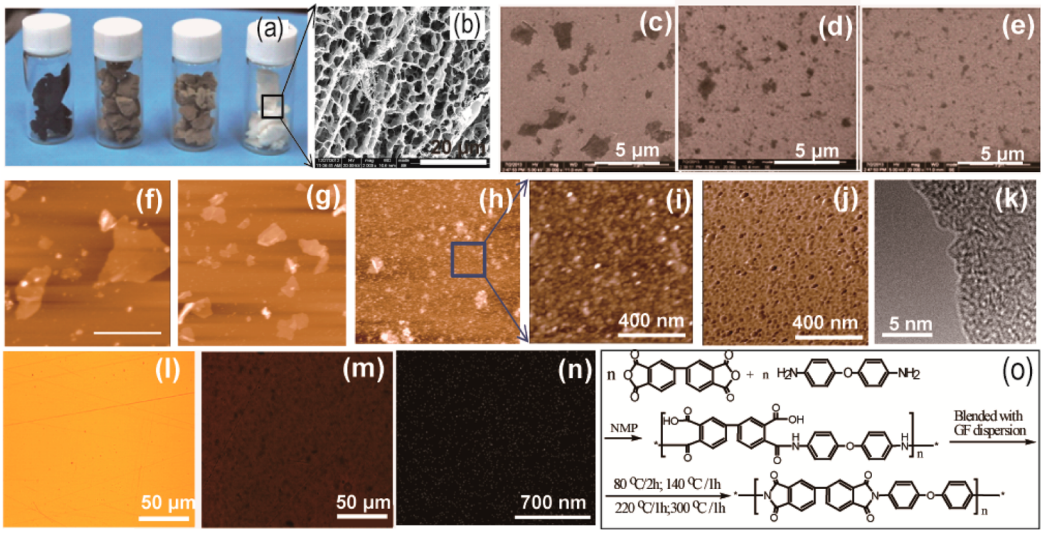

Figure 2. (a) Photographs of non-fluorinated and fluorinated graphene: neat SG, FSG-1, FSG-2, and FSG-3 (left to right). (b) SEM image of FSG-3, the alveolate structure is retained after fluorination. (c, d, e) SEM images of FSG-1, FSG-2, and FSG-3, respectively; (f, g) AFM imaging of FSG-1 and FSG-2, respectively. (h, i, j) AFM imaging and corresponding phase images of FSG-3 sheets. (k) TEM image of FSG-3, shown the single layer structure. (l, m) Optical pictures of neat polyimide films (l) and hybrids containing FSG-3 (m) under the transmission mode. (n) F-mapping of energy dispersive spectrometry (EDS) of FSG-3 hybrid. (o) Scheme for preparing the polyimide of BPDA/ODA.

Table 1. Chemical Composition and Thermal Stability of Fluorinated and Non-Fluorinated SG Measured by XPS

	chemical composition measured by XPS					
sample notation	F (at %) ± 0.2	O (at %) ± 0.2	C (at %) ± 0.2	F/C	chemical formula	mass loss peak temp. (°C)
SG	0.0	4.6	95.4	0.0	$C_1O_{0.05}$	
FSG-1	34.0	9.4	56.6	0.65	$C_1F_{0.60}O_{0.17}$	399.1
FSG-2	40.9	6.5	52.6	0.84	$C_1F_{0.78}O_{0.12}$	418.5
FSG-3	48.1	3.5	48.4	1.02	$C_1F_{1.00}O_{0.07}$	546.5

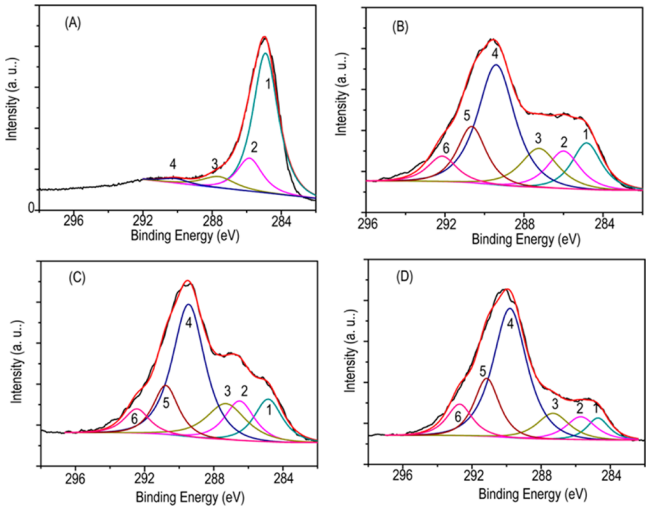

Figure 3. Curve-fitting of XPS C 1s spectrum of SG and fluorinated samples: (a) SG; (b) FSG-1; (c) FSG-2; (c) FSG-2; (d) FSG-3.

In order to observe the size of fluorographene sheets, they were deposited on the ITO glass by simple drop casting from the corresponding dilute fluorographene dispersion, which is obtained by ultrasonic dispersing in NMP for 90 min. As shown in the SEM images in Figure 2(c, d, e), the size of

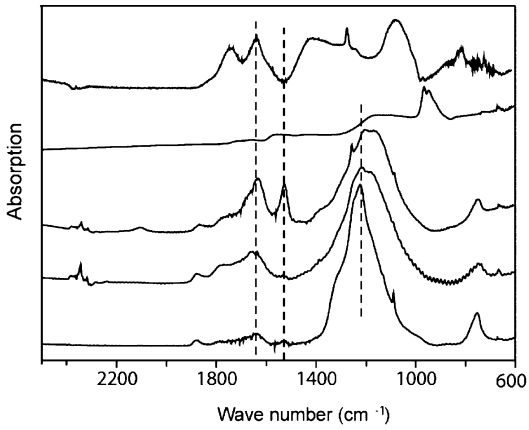

Figure 4. FTIR spectra of graphene oxide, graphene, and fluorographene: SGO, SG, FSG-1, FSG-2, and FSG-3 (top to bottom).

fluorographene sheets decreases obviously as the level of fluorination improved, while the transparency increases, indicating that the number of layers is also diminished with the aggravation of fluorination. The results of AFM imaging also confirmed this trend in Figure 2(f, g, h). For FSG-3, the number of layers is mainly in the range 1−3 and the yield of monolayered fluorographene sheet is large as shown in Supporting Information Figure S2. Its AFM picture and corresponding phase picture shown that the size of the sheets is mainly under 100 nm, indicating many FSG-3 sheets have reached the quantum scale. This not only results in a large special surface area and, consequently, a large interface for its corresponding hybrids but also may bring some unexpected results.

A 15-μm-thick FSG3 paper was prepared on a membrane filter by vacuum filtration of the FSG-3 dispersion of chloroform, being a little gray, not white as shown in Supporting Information Figure S1. The high F/C ratio enhanced hydrophobicity of fluorographene. The water contact angle in this paper is larger than 135°. Thermal gravimetric

dx.doi.org/10.1021/am5042516 | ACS Appl. Mater. Interfaces 2014, 6, 16182−16188

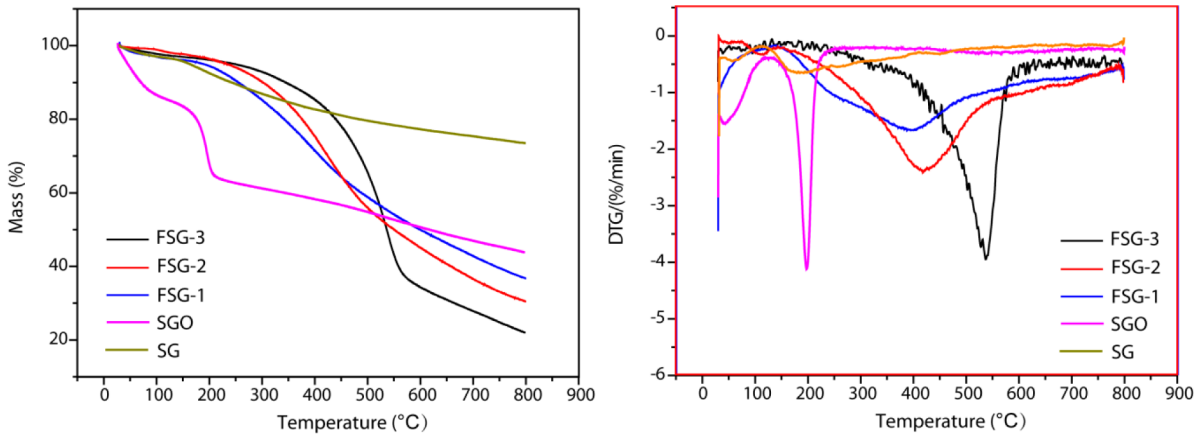

Figure 5. TGA (left) and DTA (right) lines of fluorinated samples at heating rate of 10 °C/min under N_2 atmosphere.

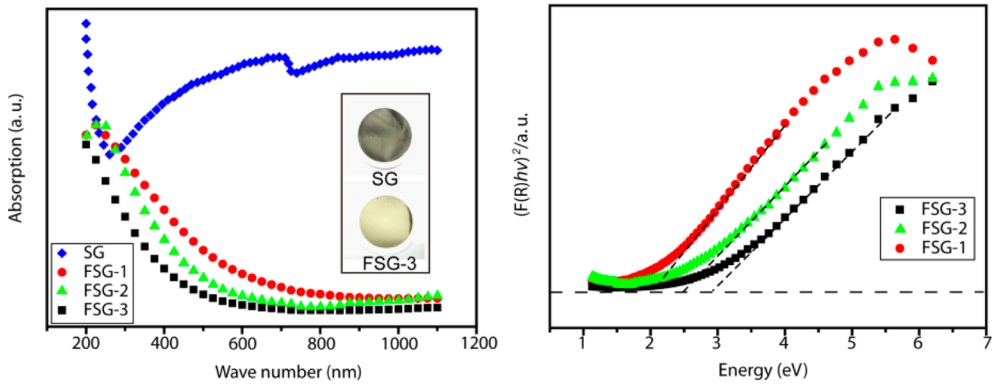

Figure 6. UV−vis diffuse reflectance spectra (left) of graphene and fluorographene papers. The inset shows the graphene and fluorographene paper from SG (graphene) and FSG-3 samples. (right) Kubulka−Munk plots of UV−vis diffuse reflectance spectra versus the band gap energies for fluorographenes. The extrapolated lines indicate the optical band gap energies of each sample.

analysis (TGA) and differential thermal analysis (DTA) results are shown in Figure 5. It can be seen that the decomposition of graphene oxide is due the elimination of oxygen related groups at around 200 °C. After chemical reduction by hydrazine, the weight loss peak at 200 °C almost disappeared. For the fluorinated samples, the weight loss peak appears and its intensity increases gradually with fluorination degree, being due to the break of C−F bond and release of volatile containing fluorine such as C_2F_6. In Table 1, the weight loss of FSG-1, FSG-2, and FSG-3 mainly occurred at 399.1, 418.5, and 546.5 °C, respectively. The decomposition temperature is well above the temperature for thermal imidization of polyimide. This is good for preserving the chemical structure of fluorographene sheets in process of preparing fluorographene/polyimide hybrids.

3.2. Dielectric Properties of Fluorographene/Polyimide Hybrids. The highly fluorinated fluorographene sheets (F/C ≈ 1) were reported with a large band gap, ~3.5 eV.[34,35] Theoretical studies have indicated that the band gap of fluorographene can be varied with changing degrees of fluorination. Two-dimensional nanostructure of fluorographene and, consequently, a large special surface area would result in a large amount of heterostructure when they are embedded into polymer matrices even at a very low filling. The dielectric confinement and strong self-polarization-induced radial localization of electronic density arising from the heterostructure between insulating and semiconducting components were likely to lead to remarkable decrease of dielectric constant.[20,36,37] Due to the strong electron-withdrawing nature and high content of fluorine atom, the fluorographene might reduce the discrete electronic levels of the hybrid system, such as the C−F bond acting on the fluorinated polyimide macromolecules. This reduces the electronic polarization of hybrids and further decreases the dielectric constant. In addition, the reduced electronic polarization and the enhanced hydrophobicity of the fluorographene sheets with high F/C ratio would prevent the polymer from moisture, reducing the water absorption. Thus, the above analysis inspired us to explore the possibility of decreasing the dielectric properties and water absorption of polyimide by incorporating fluorographene sheets.

Absorbance of nonfluorinated and fluorinated graphene (F/C = 0, 0.65, 0.84, 1.02) samples was measured by UV−vis diffuse reflectance spectroscopy, as shown in Figure 6 to obtain the band gap. The band gap energy was determined by the Kubulka-Munk method, defined as $F(R) = (1 - R)^2/(2R)$, where R is reflectance and $F(R)$ is proportional to the extinction coefficient. Figure 6 shows plots of the modified Kubulka−Munk function versus the band gap energies of fluorographene with different F/C ratio, in which the modified Kubulka−Munk function is the $F(R)$ function in terms of $h\nu$, where h is Planck's constant and ν is the light frequency. The absorbance ($F(R)$) of SG is high in the UV−vis−NR region from 200 to 1100 nm, because it has no band gap. However, the fluorographene samples have low absorbance or no absorbance in the vis−NR region, showing the band gap opening of fluorographene in this study. The band gap energy

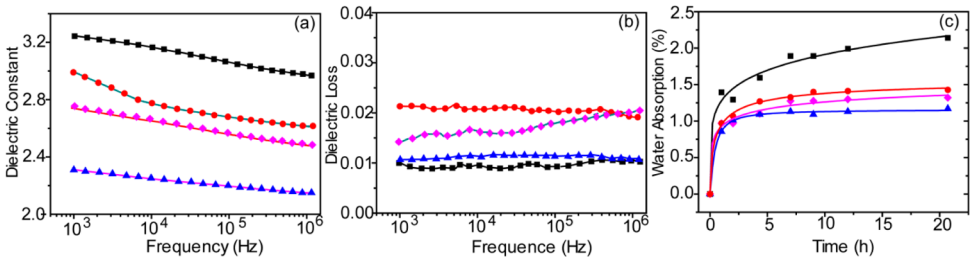

Figure 7. Dielectric properties and water absorption of the neat polyimide and fluorographene hybrid polyimide films at room temperature: (a) dielectric constant; (b) dielectric loss; and (c) water absorption. ■ neat polyimide; ● FSG-1/polyimide composite; ◆ FSG-2/polyimide composite; ▲ FSG-3/polyimide composite.

increased from 2.04 eV (FSG-1) to 2.91 eV (FSG-3) as the F/C ratio of fluorographene. This result is consistent with that of photoluminescence (PL) spectroscopy measurement shown in Supporting Information, which indicates that the higher fluorination degree of fluorographene results in the wider band gap.

The fluorographene/polyimide hybrids with a low filling (1 wt %) were synthesized, based on 3,3′,4,4′-biphenyl tetracarboxylicdiandhydride (BPDA)/4,4′-oxidianiline (ODA). The synthetic route is shown in Figure 2o. F-mapping of energy dispersive spectrometry (EDS) is an easy and convenient method to observe the dispersion of fluorographene in the hybrid films. F-mapping of EDS (Figure 2n) and optical images (Figure 2m) of hybrid film show that the fluorographene sheets were well dispersed in polymer bulk.

The dielectric constant of neat BPDA/ODA polyimide was about 3.1. The incorporation of fluorographene reduces the dielectric constant obviously as shown in Figure 7. The value is 2.8, 2.6, and 2.1 (at 1 MHz) for the corresponding hybrids of FSG-1, FSG-2, and FSG-3, respectively. Meanwhile, the values of dielectric loss of neat polyimide and hybrids are all below 0.03. In contrast to 0.011 of the neat polyimide, the value for FSG-1/polyimide and FSG-2/polyimide is slightly increased, which may be due to the existence of nonfluorinated graphene domains in the fluorographene sheets. As to nearly completely fluorinated FSG-3, the dielectric loss of its hybrid is very close to that of neat polyimide.

With the improvement of degree of fluorination, the κ-value decreased significantly. It seems that the F-content of fluorographene plays a crucial role in determining the dielectric properties of these hybrid polyimides. The amount of fluorine bonded on the two-dimension materials determines their conductivity, which affects the dielectric confinements arising from the heterostructures between these semiconductor and polyimide.[36,37] What is more, the fluorine has the strongest electron withdrawing nature of all elements by far and the reduction of discrete electronic levels at room temperature is thus expected. The trapped electron and charge confinement increase the binding energy of the hybrid films, reducing the value of the size-dependent static dielectric constant; meanwhile, the binding energy of fluorine atom bonding on the fluorographene sheets is thus decreased.[38,39] This is proved by the result of XPS analysis, as shown in Figure 8. The binding energy of F 1s decreased to 685.5 eV from 688.2 eV in polyimide matrices in contrast to that of neat fluorographene, reduced about 2.7 eV.

Initially, the introduction of fluorine into macromolecules of carbon chain polymers lowers the κ-value by increasing their free volume with a concomitant decrease in their polarizability.[40] The density of hybrid films of fluorographene/polyimide in present work increases slightly. For example, that of FSG-3 hybrid increased to 1.4106 g/cm^3 relative to 1.4029 g/cm^3 of neat polyimide film. It is evident that the change of free volume seems not to be the main reason leading to the reduction in the dielectric constant of hybrid films.

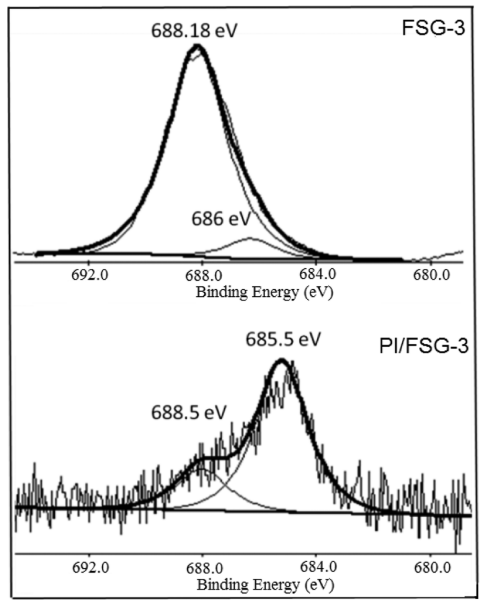

Figure 8. F 1s spectra of FSG-3 and its hybrid polyimide films; signal intensity of spectra correspond to the amount of F atom in the samples, the peak intensity of FSG is much stronger than that of fluorographene/polyimide hybrid film with only 1 wt % FSG-3.

The sheet-size of fluorographene sheets changes greatly with the improvement of fluorinated degree and consequently the special surface shows a great change, which might depend on the amount of defect. The attack of fluorine inevitably brings defects into the graphene sheets during flluorination. Under the solvent NMP and sonic conditions, the fluorographene sheets would be exfoliated and cut into "small pieces". Thus, more heterostructure was formed when FSG-3 were embedded in the polyimide matrices relative to FSG-1 and FSG-2 at the same filling fraction. However, it is uncertain whether sheet-size will affect the final dielectric properties due to the coexistence of differences of F-content. In order to show the effect of size and layer-number of fluorographene sheets on dielectric properties, the FSG-3 sheets with different morphology were prepared by controlling the ultrasonic time in the process of dispersion (Figure 9) and were composited with polyimide, respectively.

It is evident that the dielectric constant decreases significantly with increasing of ultrasonic time, as shown in Figure 10. That

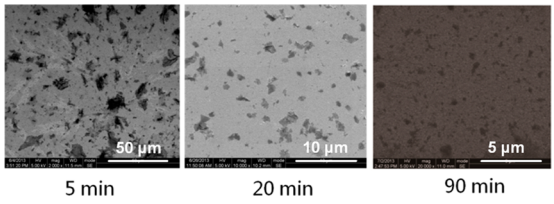

Figure 9. SEM images of the sheets of FSG-3 with different size were prepared by controlling the ultrasonic time in the process of dispersion.

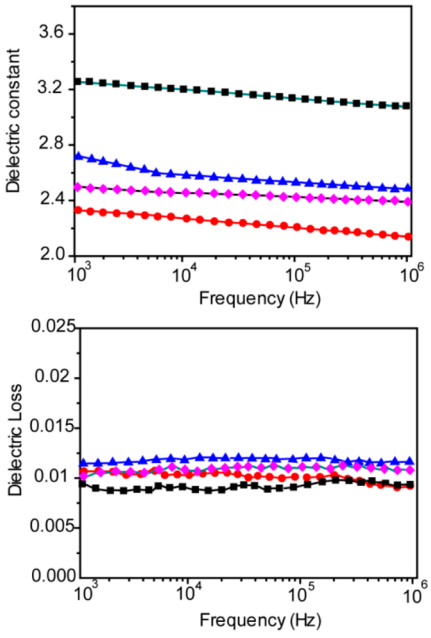

Figure 10. Dielectric properties of the neat polyimide and hybrids containing FSG-3 sheets with different size at room temperature: dielectric constant (top); dielectric loss (down). ■ neat polyimide; ▲ hybrid containing FSG-3, which is ultrasonically dispersed for 5 min; ◆ hybrid containing FSG-3 dispersed for 20 min; ● hybrid containing FSG-3 dispersed for 90 min.

is to say, a larger number of heterostructure generated a lower dielectric constant. Indisputably, the high F/C ratio and sheet-size of fluorographene sheets are both important factors that should not be neglected, but we are not sure which one is more important between them now.

The water absorption is vital for the application of polyimides in microelectronics. However, polarity has been a problem for the neat polyimides. Their typical water absorption values range from ∼2 to 4%.[41] In the present work, the value of pure BPDA/ODA polyimide is 2.2%. After incorporation of fluorographene sheets, the value of fluorographene/polyimide hybrid film obviously decreased to about 1% as shown in Figure 7c, which is very close to the lowest value reported in literatures.[41] The hydrophobicity of fluorinated graphene sheets with high F-content serves as a potential reason.[20] The network of fluorographene sheet in the polyimide matrix prevents the infiltration of moisture. The interaction between polyimide molecules and fluorographene sheets was considered as another reason. The XPS results (Figure 8) confirm the existence of this interaction, although its specific mode has not been clear. Due to the strong electron withdrawing nature and high content of fluorine atom, the fluorographene might reduce the discrete electronic levels of the hybrid system by the interaction, and further reduce the electronic polarization, which may lead to decreasing of water absorption. The diminished moisture content leads to the decreases of dielectric constant at lower frequencies, thus improving the environmental adaptability in the process of application.

In addition, the mechanical and thermal properties were studied by dynamic mechanical analysis (DMA) and TGA. The incorporation of fluorographene sheets increased the initial storage modulus E′ of the polyimide films efficiently. For instance, E′ at 40 °C for the 1 wt % FSG-3 hybrid film increased to 3.5 GPa, an increase of 120% compared to 1.6 GPa of the neat polyimide film, while their thermal stability was well maintained, as shown in Figures S4 and S5 in Supporting Information.

In summary, the incorporation of fluorographene, even at a very low filling, significantly reduced the dielectric constant and water absorption of polyimide hybrid film without sacrificing their extraordinary mechanical and thermal properties. The F/C ratio, band gap width and sheet-size of fluorographene play the important roles in determining the final properties of products. A lower κ material, even ultralow-κ, is expected to be produced via changing the polyimide matrix or increasing of fluorographene content, and this method can be extended to other polymer matrixes, which opens a novel ideas and a feasible approach to develop low-κ hybrids or other functional materials and providing a new thought to carry out the application of fluorographene as an advanced material. Further detailed studies should be carried out to more accurately exploit the mechanism of reducing dielectric constant and to develop some new functions for the fluorographene hybrids.

■ ASSOCIATED CONTENT

Supporting Information

Chemical composition of samples were analyzed by XPS; water contact angle on the FSG-3 paper; AFM imaging and thickness of FSG-3 sheets; photoluminescence (PL) spectroscopy measurement; analysis of mechanical and thermal properties of neat and hybrid polyimide films. This material is available free of charge via the Internet at http://pubs.acs.org.

■ AUTHOR INFORMATION

Corresponding Author

*Email: lxy6912@sina.com.

Notes

The authors declare no competing financial interest.

■ ACKNOWLEDGMENTS

This work was supported by the National Natural Science Foundation of China (Grant No. 50973073/50773044). We acknowledge Analytical and Testing Centre Sichuan University, China, for characterization.

■ REFERENCES

(1) Miller, R. D. In Search of Low-κ Dielectrics. *Science* **1999**, *286*, 421−423.

(2) Su, R. Q.; Muller, T. E.; Prochazka, J.; Lercher, J. A. A New Type of Low-κ Dielectric Films Based on Polysilsesquioxanes. *Adv. Mater.* **2002**, *14*, 1369−1373.

(3) Ree, M.; Yoon, J.; Heo, K. Imprinting Well-Controlled Closed-Nanopores in Spin-on Polymeric Dielectric Thin Films. *J. Mater. Chem.* **2006**, *16*, 685−697.

(4) Hedrick, J. L.; Carter, K. R.; Dipietro, R.; Miller, R. D.; Russell, T. P.; Flores, V.; Mecerreyes, D.; DuBois, P.; Jerome, R. Polyimide

Nanofoams from Aliphatic Polyester-Based Copolymers. *Chem. Mater.* **1998**, *10*, 39−49.
(5) Murotani, E.; Lee, J. K.; Chatzichristidi, M.; Zakhidov, A. A.; Taylor, P. G.; Schwartz, E. L.; Malliaras, G. G.; Ober, C. K. Cross-Linkable Molecular Glasses: Low Dielectric Constant Materials Patternable in Hydrofluoroethers. *ACS Appl. Mater. Interfaces* **2009**, *1*, 2363−2370.
(6) Maex, K.; Baklanov, M. R.; Shamiryan, D.; Iacopi, F.; Brongersma, S. H.; Yanovitskaya, Z. S. Low Dielectric Constant Materials for Microelectronics. *J. Appl. Phys.* **2003**, *93*, 8793−8841.
(7) Martin, S. J.; Godschalx, J. P.; Mills, M. E.; Shaffer, E. O.; Townsend, P. H. Development of a Low-Dielectric-Constant Polymer for The Fabrication of Integrated Circuit Interconnect. *Adv. Mater.* **2000**, *12*, 1769−1778.
(8) Maier, G. Low Dielectric Constant Polymers for Microelectronics. *Prog. Polym. Sci.* **2001**, *26*, 3−65.
(9) Huang, Y. Q.; Economy, J. New High Strength Low-κ Spin-on Thin Films for IC Application. *Macromolecules* **2006**, *39*, 1850−1853.
(10) Fu, G. D.; Shang, Z.; Hong, L.; Kang, E. T.; Neoh, K. G. Nanoporous, Ultralow-Dielectric-Constant Fluoropolymer Films from Agglomerated and Crosslinked Hollow Nanospheres of Poly (pentafluorostyrene)-block-Poly(divinylbenzene). *Adv. Mater.* **2005**, *17*, 2622−2626.
(11) Baskaran, S.; Liu, J.; Domansky, K.; Kohler, N.; Li, X. H.; Coyle, C.; Fryxell, G. E.; Thevuthasan, S.; Williford, R. E. Low Dielectric Constant Mesoporous Silica Films through Molecularly Templated Synthesis. *Adv. Mater.* **2000**, *12*, 291−294.
(12) Yang, S.; Mirau, P. A.; Pai, C. S.; Nalamasu, O.; Reichmanis, E.; Lin, E. K.; Lee, H. J.; Gidley, D. W.; Sun, J. Nanoporous Ultralow Dielectric Constant Organosilicates Templated by Triblock Copolymers. *Chem. Mater.* **2001**, *13*, 2762−2764.
(13) Huang, J. C.; Lim, P. C.; Shen, L.; Pallathadka, P. K.; Zeng, K. Y.; He, C. B. Cubic Silsesquioxane−Polyimide Nanocomposites with Improved Thermomechanical and Dielectric Properties. *Acta Mater.* **2005**, *53*, 2395−2404.
(14) Geng, Z.; Huo, M.; Mu, J.; Zhang, S.; Lu, Y.; Luan, J.; Huo, P.; Du, Y.; Wang, G. Ultra Low Dielectric Constant Soluble Polyhedral Oligomeric Silsesquioxane (POSS)-poly(aryl ether ketone) Nanocomposites with Excellent Thermal and Mechanical Properties. *J. Mater. Chem. C* **2014**, *2*, 1094−1103.
(15) Leu, C. M.; Chang, Y. T.; Wei, K. H. Polyimide-Side-Chain Tethered Polyhedral Oligomeric Silsesquioxane Nanocomposites for Low-Dielectric Film Applications. *Chem. Mater.* **2003**, *15*, 3721−3727.
(16) Li, Y.; Huang, X.; Hu, Z.; Jiang, P.; Li, S.; Tanaka, T. Large Dielectric Constant and High Thermal Conductivity in Poly (Vinylidene Fluoride)/Barium Titanate/Silicon Carbide Three-phase Nanocomposites. *ACS Appl. Mater. Interfaces* **2011**, *3*, 4396−4403.
(17) Purushothaman, R.; Palanichamy, M.; Mohammed, B. I. Functionalized KIT-6/Terpolyimide Composites with Ultra-Low Dielectric Constant. *J. Appl. Polym. Sci.* **2014**, *131*, 40508−40514.
(18) Zhang, Y. H.; Lu, S. G.; Li, Y. Q.; Dang, Z. M.; Xin, J. H.; Fu, S. Y.; Li, G. T.; Guo, R. R.; Li, L. F. Novel Silica Tube/Polyimide Composite Films with Variable Low Dielectric Constant. *Adv. Mater.* **2005**, *17*, 1056−1059.
(19) Chen, H.; Xie, L.; Lu, H.; Yang, Y. Ultra-Low-κ Polyimide Hybrid Films via Copolymerization of Polyimide and Polyoxometalates. *J. Mater. Chem.* **2007**, *17*, 1258−1261.
(20) Wahab, M. A.; Mya, K. Y.; He, C. Synthesis, Morphology, and Properties of Hydroxyl Terminated-POSS/Polyimide Low-k Nanocomposite Films. *J. Polym. Sci., Part A: Polym.Chem.* **2008**, *46*, 5887−5896.
(21) Nair, R. R.; Ren, W.; Jalil, R.; Riaz, I.; Kravets, V. G.; Britnell, L.; Blake, P.; Schedin, F.; Mayorov, A. S.; Yuan, S.; Katsnelson, M. I.; Cheng, H. M.; Strupinski, W.; Bulusheva, L. G.; Okotrub, A. V.; Grigorieva, I. V.; Grigorenko, A. N.; Novoselov, K. S.; Geim, A. K. Fluorographene: A Two-Dimensional Counterpart of Teflon. *Small* **2010**, *6*, 2877−2885.
(22) Zbořil, R.; Karlický, F.; Bourlinos, A. B.; Steriotis, T. A.; Stubos, A. K.; Georgakilas, V.; Šafářová, K.; Jančík, D.; Trapalis, C.; Otyepka, M. Graphene Fluoride: A Stable Stoichiometric Graphene Derivative and Its Chemical Conversion to Graphene. *Small* **2010**, *6*, 2885−2891.
(23) Novoselov, K. S.; Jiang, D.; Schedin, F.; Booth, T. J.; Khotkevich, V. V.; Morozov, S. V.; Geim, A. K. Two-Dimensional Atomic Crystals. *P. Natl. Acad. Sci. U.S.A.* **2005**, *102*, 10451−10453.
(24) Schrier, J. Fluorinated and Nanoporous Graphene Materials as Sorbents for Gas Separations. *ACS Appl. Mater. Interfaces* **2011**, *3*, 4451−4458.
(25) Mondal, T.; Bhowmick, A. K.; Krishnamoorti, R. Stress Generation and Tailoring of Electronic Properties of Expanded Graphite by Click Chemistry. *ACS Appl. Mater. Interfaces* **2014**, *6*, 7244−7253.
(26) Robinson, J. T.; Burgess, J. S.; Junkermeier, C. E.; Badescu, S. C.; Reinecke, T. L.; Perkins, F. K.; Zalalutdniov, M. K.; Baldwin, J. W.; Culbertson, J. C.; Sheehan, P. E.; Snow, E. S. Properties of Fluorinated Graphene Films. *Nano Lett.* **2010**, *10*, 3001−3004.
(27) Withers, F.; Russo, S.; Dubois, M.; Craciun, M. Nanopatterning of Fluorinated Graphene by Electron Beam Irradiation. *Nanoscale Res. Lett.* **2011**, *6*, 526−536.
(28) Kwon, S.; Ko, J. H.; Jeon, K. J.; Kim, Y. H.; Park, J. Y. Enhanced Nanoscale Friction on Fluorinated Graphene. *Nano Lett.* **2012**, *12*, 6043−6048.
(29) Li, Y.; Li, F.; Chen, Z. Graphane/Fluorographene Bilayer: Considerable C−H···F−C Hydrogen Bonding and Effective Band Structure Engineering. *J. Am. Chem. Soc.* **2012**, *134*, 11269−11275.
(30) Wang, X.; Dai, Y. Y.; Gao, J.; Huang, J. Y.; Li, B. Y.; Fan, C.; Yang, J.; Liu, X. Y. High-Yield Production of Highly Fluorinated Graphene by Direct Heating Fluorination of Graphene-Oxide. *ACS Appl. Mater. Interfaces* **2013**, *5*, 8294−8299.
(31) Hirata, M.; Gotou, T.; Horiuchi, S.; Fujiwara, M.; Ohba, M. Thin-film Particles of Graphite Oxide 1: High-yield Synthesis and Flexibility of The Particles. *Carbon* **2004**, *42*, 2929−2937.
(32) Becerril, H. A.; Mao, J.; Liu, Z.; Stoltenberg, R. M.; Bao, Z.; Chen, Y. Evaluation of Solution-Processed Reduced Graphene Oxide Films As Transparent Conductors. *ACS Nano* **2008**, *2*, 463−470.
(33) Wang, Y.; Shi, Z.; Huang, Y.; Ma, Y.; Wang, C.; Chen, M.; Chen, Y. Supercapacitor Devices Based on Graphene Materials. *J. Phys. Chem. C* **2009**, *113*, 13103−13107.
(34) Shen, N.; Sofo, J. O. Dispersion of Edge States and Quantum Confinement of Electrons in Graphene Channels Drawn on Graphene Fluoride. *Phys. Rev. B* **2011**, *83*, 245424−245430.
(35) Jeon, K. J.; Lee, Z.; Pollak, E.; Moreschini, L.; Bostwick, A.; Park, C. M.; Mendelsberg, R.; Radmilovic, V.; Kostecki, R.; Richardson, T. J.; Rotenberg, E. Fluorographene: A Wide Bandgap Semiconductor with Ultraviolet Luminescence. *ACS Nano* **2011**, *5*, 1042−1046.
(36) Tsu, R.; Babic, D. Doping of a Quantum Dot. *Appl. Phys. Lett.* **1994**, *64*, 1806−1808.
(37) Fonoberov, V. A.; Pokatilov, E. P.; Balandin, A. A. Exciton States and Optical Transitions in Colloidal CdS Quantum Dots: Shape and Dielectric Mismatch Effects. *Phys. Rev. B* **2002**, *66*, 085310−085322.
(38) Glezos, N.; Argitis, P.; Velessiotis, D.; Diakoumakos, C. D. Tunneling Transport in Polyoxometalate Based Composite Materials. *Appl. Phys. Lett.* **2003**, *83*, 488−490.
(39) Movilla, J. L.; Planelles, J. Off-centering of Hydrogenic Impurities in Quantum Dots. *Phys. Rev. B* **2005**, *71*, 075319−075325.
(40) Hougham, G.; Tesoro, G.; Shaw, I. Influence of Free Volume Change on the Relative Permittivity and Refractive Index in Fluoropolyimides. *Macromolecules* **1994**, *27*, 3642−2649.
(41) Willi, V.; Robert, D. M.; Geraud, D. Low Dielectric Constant Materials. *Chem. Rev.* **2010**, *110*, 56−110.